Ubiquitin binding by the CUE domain promotes endosomal localization of the Rab5 GEF Vps9

Tess Shideler[a], Daniel P. Nickerson[b], Alexey J. Merz[b], and Greg Odorizzi[a]
[a]Department of Molecular, Cellular, and Developmental Biology, University of Colorado, Boulder, CO 80309-0347;
[b]Department of Biochemistry, University of Washington, Seattle, WA 98195-3750

ABSTRACT **Vps9 and Muk1 are guanine nucleotide exchange factors (GEFs) in *Saccharomyces cerevisiae* that regulate membrane trafficking in the endolysosomal pathway by activating Rab5 GTPases. We show that Vps9 is the primary Rab5 GEF required for biogenesis of late endosomal multivesicular bodies (MVBs). However, only Vps9 (but not Muk1) is required for the formation of aberrant class E compartments that arise upon dysfunction of endosomal sorting complexes required for transport (ESCRTs). ESCRT dysfunction causes ubiquitinated transmembrane proteins to accumulate at endosomes, and we demonstrate that endosomal recruitment of Vps9 is promoted by its ubiquitin-binding CUE domain. Muk1 lacks ubiquitin-binding motifs, but its fusion to the Vps9 CUE domain allows Muk1 to rescue endosome morphology, cargo trafficking, and cellular stress-tolerance phenotypes that result from loss of Vps9 function. These results indicate that ubiquitin binding by the CUE domain promotes Vps9 function in endolysosomal membrane trafficking via promotion of localization.**

Monitoring Editor
Sandra Lemmon
University of Miami

Received: Jun 26, 2014
Revised: Jan 29, 2015
Accepted: Feb 2, 2015

INTRODUCTION

Rab GTPases control intracellular membrane-trafficking pathways in eukaryotes by recruiting distinct sets of effector proteins to specific membrane microdomains. Rab effectors include proteins that promote transport vesicle budding, adaptor proteins that coordinate vesicle/organelle motility along the cytoskeleton, and tethering proteins that facilitate assembly of *trans*-SNARE complexes required to drive membrane fusion reactions (reviewed in Stenmark, 2009). Rabs bound to GTP associate with membranes stably and adopt an active conformation capable of binding effector proteins, whereas Rabs bound to GDP generally do not bind effectors and are vulnerable to extraction from the membrane. The activation state of Rabs is controlled by guanine nucleotide exchange factors (GEFs) and GTPase-accelerating proteins (GAPs). GEFs activate Rabs by stimulating GDP release so that GTP can bind. GAPs accelerate the intrinsically low rate of GTP hydrolysis by Rabs, thereby switching them to their inactive, GDP-bound state (Barr and Lambright, 2010). The specific intracellular localization patterns of GEFs and GAPs therefore determine the spatiotemporal activities of Rabs along membrane-trafficking pathways, although factors that specify localizations of GEFs and GAPs are incompletely understood.

VPS9-domain proteins constitute a large family of GEFs with specificity toward Rab5 and related Rabs. Mammals have >20 VPS9 paralogues, the best characterized of which is the Rabex-5 GEF, which activates Rab5A at early endosomes (Horiuchi *et al.*, 1997). Rab5A promotes homotypic fusion between early endosomes, as well as fusion between early endosomes and endocytic transport vesicles (Grovel *et al.*, 1991; Rubino *et al.*, 2000). Rabex-5 is recruited to early endosomes, in part, through a pair of tandem ubiquitin-binding domains (A20-like Zn finger and MIU motifs; Mattera and Bonifacino, 2008). *Saccharomyces cerevisiae* has two VPS9-domain proteins, Vps9 and Muk1, both of which have GEF activity in vitro toward all three members of the yeast Rab5 subfamily (Hama *et al.*, 1999; Cabrera *et al.*, 2013; Paulsel *et al.*, 2013). In vivo, deletion of the *VPS9* gene causes obvious endolysosomal membrane trafficking defects that are exacerbated by simultaneous deletion of *MUK1*, but phenotypes caused by deletion of *MUK1* alone are largely undetectable (Burd *et al.*, 1996; Paulsel *et al.*, 2013). Like mammalian Rabex-5, yeast Vps9 binds directly to ubiquitin but does so via its C-terminal CUE domain (Davies *et al.*, 2003; Donaldson *et al.*, 2003; Prag *et al.*, 2003; Shih *et al.*, 2003), whereas Muk1 lacks

This article was published online ahead of print in MBoC in Press (http://www.molbiolcell.org/cgi/doi/10.1091/mbc.E14-06-1156) on February 11, 2015.

Address correspondence to: Greg Odorizzi (odorizzi@colorado.edu), Daniel P. Nickerson (dpn2@u.washington.edu).

Abbreviations used: EM, electron microscopy; ESCRT, endosomal sorting complex required for transport; GEF, guanine nucleotide exchange factor; ILV, intraluminal vesicle; MVB, multivesicular body.

motifs implicated in binding ubiquitin. Vps9 function in vivo is not strongly affected by disabling its interaction with ubiquitin (Davies *et al.*, 2003; Prag *et al.*, 2003), raising the possibility that the CUE domain has an autoinhibitory role. Indeed, Vps9 GEF activity in vitro is enhanced by point mutation of the CUE domain (Keren-Kaplan *et al.*, 2012), but how this domain might regulate Vps9 function is unknown.

Like their GEFs, the three Rab5 paralogues in yeast (Vps21, Ypt52, and Ypt53) have partially redundant functions, but the loss of Vps21 alone is responsible for causing the major endolysosomal trafficking defects that occur in the absence of Rab5 activity (Singer-Krüger *et al.*, 1994; Nickerson *et al.*, 2012, Cabrera *et al.*, 2013). Vps21 is required for efficient membrane trafficking to the lysosomal vacuole in yeast (Burd *et al.*, 1996) and has a major role in the maturation of early endosomes into late endosomal multivesicular bodies (MVBs; Nickerson *et al.*, 2012; Russell *et al.*, 2012). MVBs contain intralumenal vesicles (ILVs) that are formed by the activities of endosomal sorting complexes required for transport (ESCRTs; reviewed in Hanson and Cashikar, 2012). ESCRTs also sort ubiquitinated transmembrane proteins into ILVs, and both the ILVs and their protein cargoes are degraded when MVBs fuse with lysosomes/vacuoles. A severe reduction in MVB biogenesis occurs upon disruption of Vps21 but not other Rab5 paralogues in yeast (Russell *et al.*, 2012), pointing to a specific role for Vps21 in directing endosomal maturation, but a mechanistic link between ESCRT-mediated protein sorting and Vps21 activity has not been defined.

Mutations that disrupt ESCRT functions inhibit normal endosomal maturation, instead causing the formation of class E compartments, which are enlarged and aberrantly flattened endosomes stacked against one another (Rieder *et al.*, 1996). ESCRT dysfunction also causes Vps21 hyperactivation, which is responsible for the up-regulation of endosomal membrane fusion activity that drives the characteristic enlargement of class E compartments (Russell *et al.*, 2012). Like Vps21, Vps9 aberrantly accumulates at class E compartments when ESCRT function is compromised, but Muk1 is absent from these abnormal structures (Russell *et al.*, 2012; Paulsel *et al.*, 2013). These observations suggest the hypothesis that ESCRT dysfunction drives Vps21 hyperactivation and concomitant class E compartment formation through enhanced Vps9 activity. We show that formation of class E compartments requires Vps9 and that the Vps9 CUE domain drives accumulation of Vps9 at these aberrant endosomal structures through its interactions with ubiquitin. Fusion of the Vps9 CUE domain to Muk1 results in localization of the chimera to endosomal membranes and rescues phenotypes resulting from loss of Vps9 function. These results support a model in which the Vps9 CUE domain serves as a localization determinant by binding ubiquitinated transmembrane proteins at endosomes to ensure that Vps21 activation is sustained during endosomal maturation.

RESULTS

Vps9 is the yeast Rab5 GEF that drives the biogenesis of late endosomal compartments

Genetic studies indicated that Rab5 activity is required for biogenesis of MVBs (Nickerson *et al.*, 2012; Russell *et al.*, 2012) and that Vps9 is key to enabling Rab5-dependent membrane trafficking in the endolysosomal pathway, with Muk1 playing an auxiliary role (Paulsel *et al.*, 2013). Therefore we tested by electron microscopy (EM) the requirement for Vps9 versus Muk1 in MVB biogenesis. Previous EM studies of yeast in which the *VPS9* gene had been deleted (*vps9*Δ) examined cells that had been preserved at room temperature with chemical fixatives (Burd *et al.*, 1996; Cabrera *et al.*, 2013), which can be suitable for general comparisons of cellular morphologies but is suboptimal for evaluating endosomes due to the dynamic nature of these organelles. In contrast, preparation of yeast for EM by high-pressure freezing and low-temperature fixation improves the preservation of organelle ultrastructure (Giddings *et al.*, 2001), including MVBs in wild-type yeast and class E compartments in ESCRT-mutant cells (Luhtala and Odorizzi, 2004). The abundance of MVBs we observed by EM of high-pressure-frozen wild-type yeast (Figure 1, A and D) was not dramatically altered in *muk1*Δ cells (Figure 1, B and D), whereas *vps9*Δ cells had an obvious reduction in the frequency of MVBs (Figure 1, C and D). That the deletion of *VPS9* does not completely eliminate MVB biogenesis but substantially cripples this process is in agreement with previous findings that sorting of ILV cargoes is much reduced but persists in the absence of Vps9 (Paulsel *et al.*, 2013) or when Vps21 Rab5 activity is absent (Nickerson *et al.*, 2012; Russell *et al.*, 2012).

We also tested by EM whether Vps9, like Vps21, is essential for the formation of aberrantly flattened and stacked endosomal membranes (class E compartments) seen in ESCRT-mutant cells. Indeed, the characteristic class E compartment morphology seen in cells lacking the regulatory Vps4 ATPase of the ESCRT pathway (*vps4*Δ; Figure 1E) was not observed in double-mutant cells lacking both Vps4 and Vps9 (*vps4*Δ *vps9*Δ; Figure 1, G and H). In contrast, Muk1 has no apparent role in the formation of class E compartments, since neither the morphology (Figure 1F) nor the abundance (Figure 1H) of these aberrant endosomal structures was altered by deletion of the *MUK1* gene in *vps4*Δ cells. Along with our observation that Vps9 is more important than Muk1 in MVB biogenesis (Figure 1D), these results show that Vps9 but not Muk1 plays a critical role in the biogenesis of late endosomal compartments.

CUE-domain binding to ubiquitin drives Vps9 accumulation at class E compartments

Mammalian Rabex-5 binds ubiquitin with two independent ubiquitin-binding motifs (A20-like Zn finger and MIU motifs) oriented in tandem near its N-terminus (Mattera *et al.*, 2006). Mutations that disable its binding to ubiquitin strongly reduce Rabex-5 endosomal localization, suggesting a model in which its endosomal recruitment is mediated through interaction with ubiquitinated transmembrane proteins trafficking through the endolysosomal pathway (Mattera and Bonifacino, 2008). Whether ubiquitin binding by the Vps9 CUE domain has a similar role in promoting the endosomal recruitment of yeast Vps9 had not yet been addressed. Thus we compared the localizations of green fluorescent protein (GFP) fused to wild type and mutant derivatives of Vps9 in yeast by fluorescence microscopy. Using a chromosomal integration of C-terminally tagged Vps9-GFP expressed at endogenous Vps9 levels, we previously reported that Vps9 appears predominantly cytosolic in wild-type yeast but accumulates at class E compartments in ESCRT-mutant cells (Russell *et al.*, 2012). We observed a similar localization pattern when N-terminally tagged GFP-Vps9 was overexpressed from a high-copy (2 μ) plasmid in wild-type cells (Figure 2A) versus *vps4*Δ cells (Figure 2B), both of which were stained with FM 4-64, a lipophilic dye that labels vacuolar membranes and class E compartments (Vida and Emr, 1995). These observations suggest that endosomal association of Vps9 is dynamic and that ESCRT dysfunction either inhibits Vps9 dissociation from endosomes or promotes its association. We used GFP-tagged Vps9 mutants to determine which domains of Vps9 are required for its enrichment at class E compartments in *vps4*Δ cells. To facilitate this analysis, we overexpressed GFP-Vps9 mutant derivatives in *vps4*Δ cells that also express endogenous wild-type Vps9, thereby guarding against

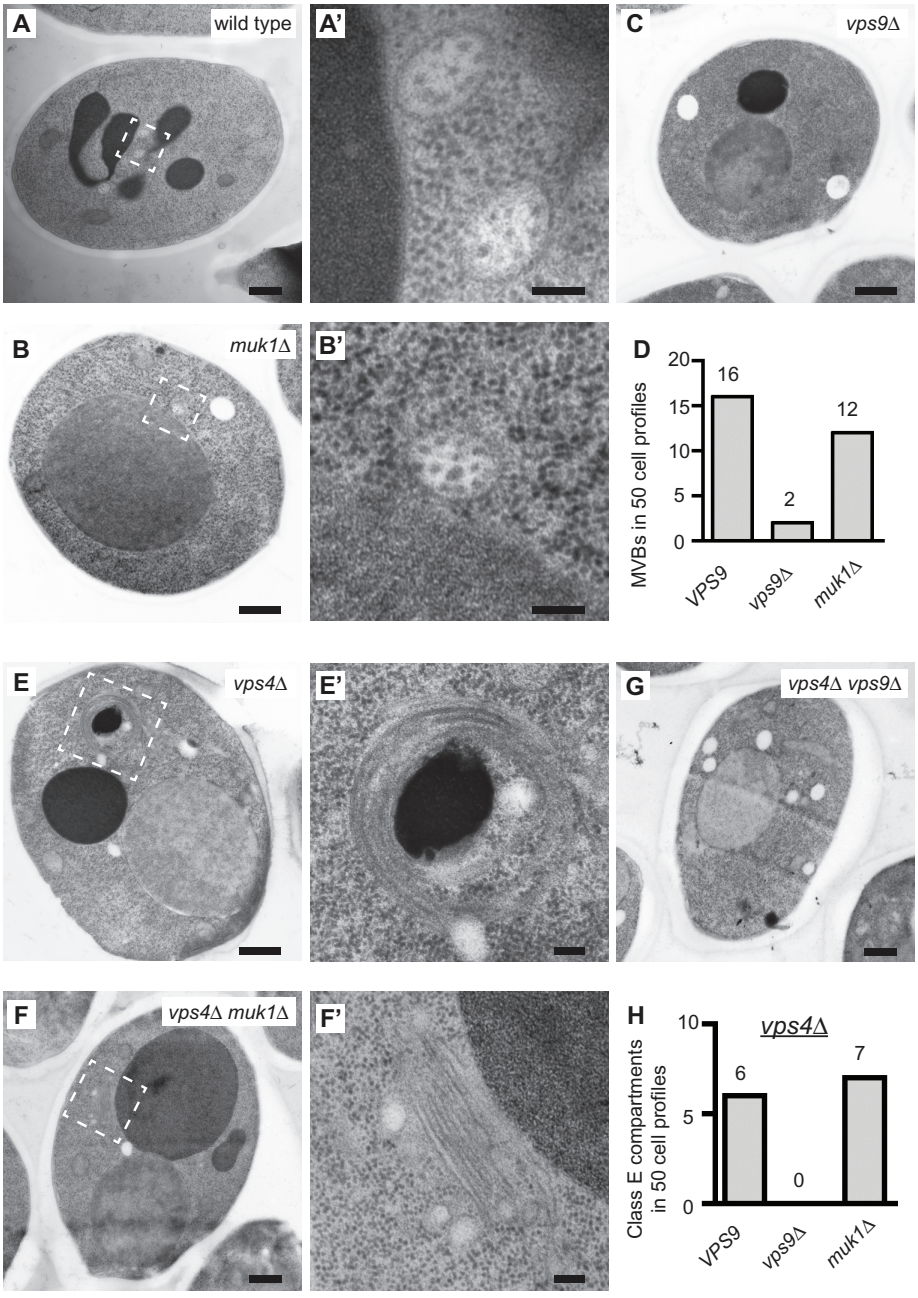

FIGURE 1: Vps9 is the yeast Rab5 GEF that drives the biogenesis of late endosomal compartments. (A–C, E–G) Electron micrographs; A′, B′, E′, and F′ show higher magnification of MVBs or class E compartments. Bars, 100 nm (A′, B′, E′, F′), 500 nm (A, B, C, E, F, G). (D, H) Quantification of MVBs or class E compartments in 50 cell profiles.

the possibility that an apparent reduction in class E compartment localization was due to a loss of Vps9 function required for class E compartment formation. To compare the distribution of Vps9 mutants in *vps4*Δ cells, we measured the fluorescence intensity of GFP at FM 4-64–labeled perivacuolar class E compartment structures. To account for varying expression levels between individual cells, we expressed the level of localization to class E compartments as a ratio of the mean fluorescence intensity (F_R) at FM 4-64–labeled structures to the mean fluorescence intensity of an area of cytosol (Figure 2J).

Because ubiquitinated transmembrane proteins accumulate at class E compartments in response to ESCRT dysfunction (Ren *et al.*, 2008), we speculated that the concentration of GFP-Vps9 at class E compartments is driven by the ubiquitin-binding Vps9 CUE domain. Indeed, GFP fused to only the CUE domain of Vps9 localized to class E compartments (Figure 2C) as strongly as it did when fused to full-length Vps9 (Figure 2B; $F_R = 3.29 \pm 0.21$ vs. 3.53 ± 0.36, respectively). In contrast, the GFP-CUE fusion protein appeared entirely cytosolic upon introduction of the $M_{419}D$ point mutation (Figure 2D; $F_R = 0.96 \pm 0.03$), which disables the CUE domain from binding ubiquitin (Davies *et al.*, 2003; Prag *et al.*, 2003). Thus GFP-CUE recruitment to class E compartments can be mediated through its binding to ubiquitin.

Disabling the interaction of full-length GFP-Vps9 with ubiquitin by the $M_{419}D$ point mutation in the CUE domain (*vps9*^{M419D}; Figure 2E) or by deletion of the CUE domain (*vps9*Δ^{CUE}; Figure 2F) caused a shift to the cytosol similar to that of GFP-CUE^{M419D} ($F_R = 1.35 \pm 0.07$ and 1.18 ± 0.05, respectively). We occasionally saw these ubiquitin-binding-defective Vps9 mutants localize weakly to class E compartments, but the difference in mean fluorescence ratio between either GFP-vps9Δ^{CUE} or GFP-vps9^{M419D} versus GFP-CUE^{M419D} was not significant by Bonferroni posthoc test. Cells expressing GFP fused to the central VPS9 domain (VND) or the flanking Vps9 N-terminus (NT) showed no detectable GFP localization to class E compartments ($F_R = 0.99 \pm 0.03$ and 0.91 ± 0.04). Therefore Vps9 is enriched at class E compartments by the CUE domain interacting with ubiquitin.

Ubiquitin binding by Vps9 is not required for MVB or class E compartment biogenesis

Disruption of Vps9 CUE-domain binding to ubiquitin causes little or no apparent defect in the sorting of ILV cargoes at MVBs (Davies *et al.*, 2003; Prag *et al.*, 2003), and our EM analysis confirmed the presence of MVBs in yeast in which the wild-type *VPS9* gene was replaced either by *vps9*^{M419D} or by the truncated *vps9*Δ^{CUE} allele expressed from a low-copy (*CEN*) plasmid (Figure 3A). Surprisingly, we observed no suppression of class E compartments in *vps4*Δ cells expressing either *vps9*^{M419D} or *vps9*Δ^{CUE} in place of wild-type *VPS9* (Figure 3B), despite the loss in Vps9 endosomal localization caused by mutation of the CUE domain (Figure 2). Unlike deletion of the *VPS9* gene, therefore, mutations that disable Vps9 binding to ubiquitin have no apparent effect on either normal late endosomal biogenesis or abnormal accumulation of membrane in ESCRT-mutant cells. Based on the observation from in vitro studies suggesting that Vps9 is autoinhibited by interaction of its CUE domain with ubiquitin (Keren-Kaplan *et al.*, 2012), our EM results are consistent with

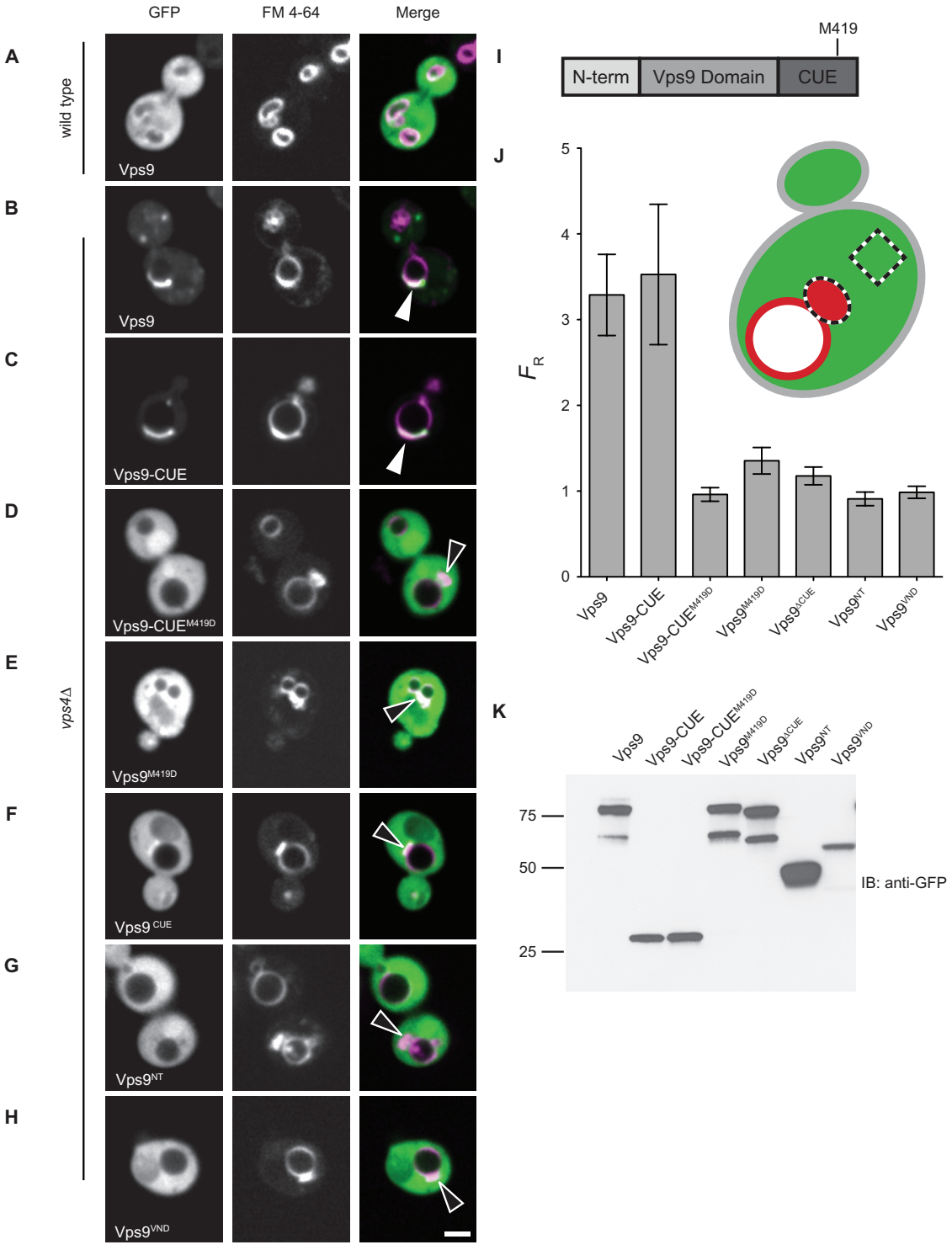

FIGURE 2: CUE-domain binding to ubiquitin drives Vps9 accumulation at class E compartments. Confocal fluorescence micrographs of FM 4-64–stained cells expressing GFP-tagged versions of Vps9 from a high-copy (2 μ) plasmid in wild-type (A) and *vps4*Δ (B–H) cells. Arrowheads indicate FM 4-64–labeled class E compartments at which GFP either does (closed arrowheads) or does not (open arrowheads) colocalize. Bar, 2 μm. (I) Model of Vps9 domains. (J) Fluorescence intensity ratio (F_R) of GFP localization at class E compartments relative to cytosol. Error bars are 95% confidence interval from at least 10 cells. (K) Western blot of total yeast cell extracts showing expression of mutant GFP-Vps9 proteins. IB, immunoblot.

the possibility that the loss of endosomal localization of Vps9 mutated in its CUE domain might be offset by an increase in its GEF activity so that activation of Vps21 by Vps9 is sustained for the biogenesis of MVBs under otherwise normal conditions and during class E compartment biogenesis upon ESCRT dysfunction.

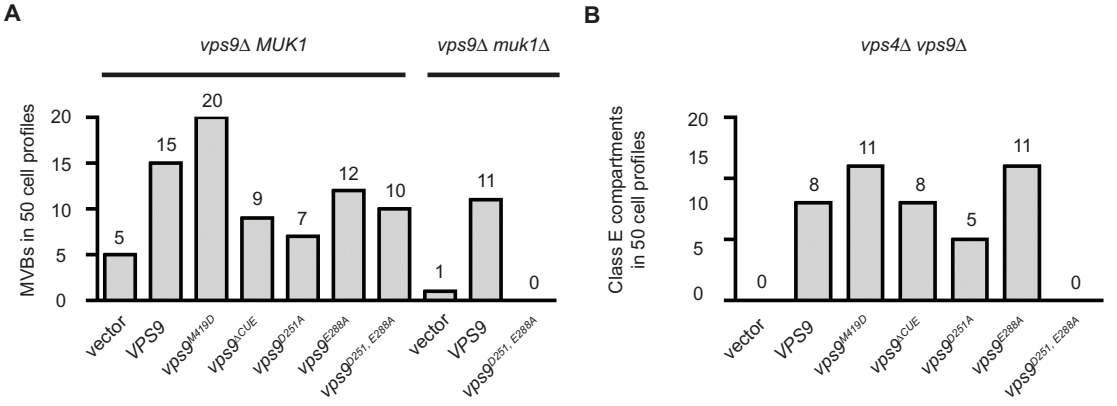

FIGURE 3: Ubiquitin binding by Vps9 is not required for MVB or class E compartment biogenesis. EM quantification of the number of MVBs (A) or class E compartments (B) in 50 cell profiles of *vps9*Δ or *vps9*Δ *muk1*Δ cells transformed with low-copy (*CEN*) plasmids expressing the indicated *vps9* alleles.

GEF-deficient Vps9 supports MVB biogenesis but not class E compartment formation

Based on structural studies of Vps9 homologues in mammalian cells (Rabex-5; Delprato *et al.*, 2004) and in *Arabidopsis* (Vps9a; Uejima *et al.*, 2010), Asp_{251} in yeast Vps9 was predicted to have a direct role in stimulating nucleotide exchange by promoting GDP dissociation from Vps21, whereas Glu_{288} in Vps9 was predicted to function indirectly by stabilizing the GEF:Rab interface. In vitro studies confirmed that Ala substitution at Asp_{251} or Glu_{288} reduces yeast Vps9 nucleotide exchange activity toward Vps21 (Delprato *et al.*, 2004; Keren-Kaplan *et al.*, 2012), but complete elimination of nucleotide exchange requires simultaneous substitution of both residues (Keren-Kaplan *et al.*, 2012). Consistent with this pattern of reduction in Vps9 GEF activity in vitro, we observed in vivo that the formation of class E compartments in *vps4*Δ cells was not disabled by expressing either $vps9^{D251A}$ or $vps9^{E288A}$ in place of wild-type *VPS9*, but class E compartment formation was completely blocked in *vps4*Δ cells expressing the double-mutant $vps9^{D251A,E288A}$ allele (Figure 3B). Thus the requirement for Vps9 in class E compartment formation correlates with its nucleotide exchange activity, which is consistent with Vps9 driving accumulation of aberrant endosomal membrane through the activation of Vps21.

Although the double point-mutant $vps9^{D251A,E288A}$ allele abolished class E compartment formation (Figure 3B), it did not totally eliminate MVB biogenesis (Figure 3A), which was not surprising, given that MVB biogenesis is reduced but not eliminated in *vps9*Δ cells (Figures 1A and 3A). The basal rate of MVB biogenesis in the absence of Vps9 function is likely sustained by Muk1 activity, because MVBs were absent from *vps9*Δ *muk1*Δ cells expressing *vps9* alleles lacking GEF activity (Figure 3A). Taken together, these data suggest that, without Vps9 GEF activity, late endosome biogenesis is maintained by residual Rab5 stimulation by Muk1. In contrast, class E compartment formation under conditions of ESCRT dysfunction specifically requires Vps9 GEF activity to stimulate Vps21 hyperactivity that drives endosomal membrane accumulation beyond what is normally required for normal late endosome biogenesis (Russell *et al.*, 2012).

The CUE and GEF domains have distinct roles in Vps9 function

Owing to their partial functional redundancies, the three yeast Rab5 paralogues (Vps21, Ypt52, and Ypt53) must be disrupted in combination in order to discern many of the phenotypes that stem from insufficient Rab5 signaling (Singer-Krüger *et al.*, 1994; Nickerson *et al.*, 2012). The Rab5 GEFs, Vps9 and Muk1, exhibit similar partial redundancies that necessitate their combined disruption in order to fully phenocopy the loss of Rab5 signaling (Figure 3; Cabrera *et al.*, 2013; Paulsel *et al.*, 2013). Therefore the functional contributions of the Vps9 CUE and GEF domains were examined in the context of *vps9*Δ cells versus *vps9*Δ *muk1*Δ cells expressing CUE- or GEF-mutant *vps9* alleles.

We first tested thermotolerance because loss of Rab5 activity causes temperature-sensitive cell growth (Singer-Krüger *et al.*, 1994; Nickerson *et al.*, 2012). At 37°C, *vps9*Δ cells displayed an obvious growth defect that was exacerbated in *vps9*Δ *muk1*Δ cells, but the growth of both strains at 37°C was fully restored by low-copy expression of $vps9^{M419D}$ or $vps9\Delta^{CUE}$ (Figure 4A). Ubiquitin binding by the CUE domain is therefore dispensable for the function Vps9 has in promoting tolerance to heat stress. Similarly, expression of the single point-mutant $vps9^{D251A}$ and $vps9^{E288A}$ alleles fully rescued growth of *vps9*Δ and *vps9*Δ *muk1*Δ cells at 37°C, but the double point-mutant $vps9^{D251A,E288A}$ allele, which has no GEF activity in vitro (Keren-Kaplan *et al.*, 2012), only partially restored growth in *vps9*Δ cells and failed to restore growth in *vps9*Δ *muk1*Δ cells (Figure 4A). Partial rescue by $vps9^{D251A,E288A}$ in *vps9*Δ cells expressing Muk1 might indicate that Vps9 has a function unrelated to its GEF activity, in which case, Muk1 would be required to provide a basal level of GEF activity to potentiate Rab5 signaling. Alternatively, the $vps9^{D251A,E288A}$ allele might retain a residual level of GEF activity in vivo that is insufficient on its own to support effective Rab5 signaling but might augment the contribution of Muk1.

We next assayed functional contributions of the Vps9 CUE and GEF domains toward vacuolar protein sorting by examining the localization of carboxypeptidase Y (CPY), a soluble vacuolar hydrolase, which was fused to a reporter enzyme, invertase (Inv; Bankaitis *et al.*, 1986). In wild-type cells, newly synthesized CPY-Inv is sorted from the Golgi to endosomes en route to the vacuole, but *vps9*Δ cells aberrantly secrete ~50% of CPY-Inv (Raymond *et al.*, 1992; Burd *et al.*, 1996). Substantially more CPY-Inv is secreted by double-mutant cells lacking both Vps9 and Muk1 (Paulsel *et al.*, 2013), indicating that Muk1 makes a significant contribution to Rab5-dependent steps in the vacuolar protein sorting pathway, at least in the absence of Vps9. Consistent with thermotolerance results described earlier, CPY-Inv sorting defects in *vps9*Δ *muk1*Δ cells were reversed by

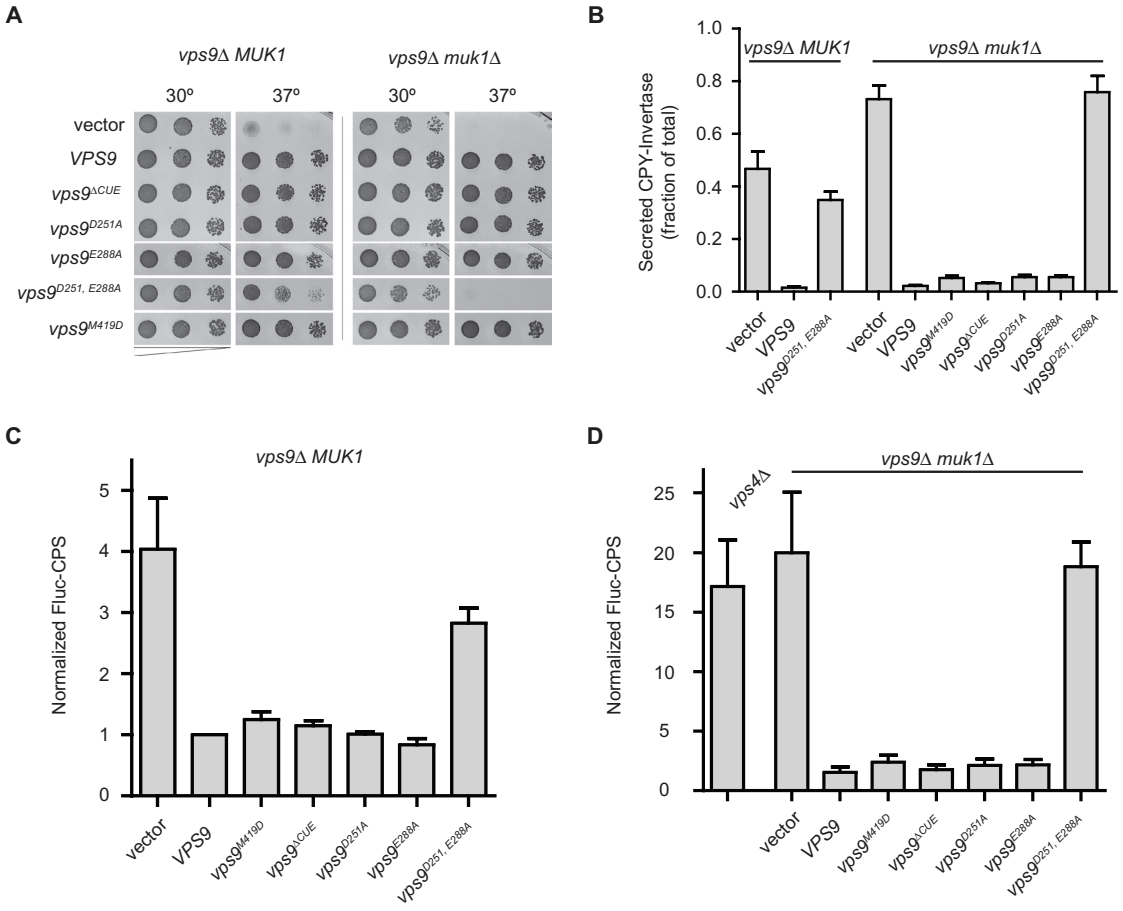

FIGURE 4: The CUE and GEF domains have distinct roles in Vps9 function. (A) Limiting dilutions of yeast after 45 h of growth on minimal synthetic agar medium at 30 vs. 37°C. (B) Analysis of a chimeric CPY-Inv reporter enzyme in extracellular and total cellular fractions. Bars represent means of four independent experiments, except for column 3, which represents three independent experiments. (C, D) LUCID analysis of FLuc-Cps1 sorting in the MVB pathway. Signal from luciferase-tagged Cps1 is inversely proportional to the efficiency of sorting into ILVs. Alleles of *VPS9* expressed from a *CEN* plasmid were analyzed for function in cells lacking only Vps9 (*vps9*Δ; C) and cells lacking both Vps9 and Muk1 (*vps9*Δ *muk1*Δ*;* D). Cells lacking Vps4 (*vps4*Δ) served as a positive control for defective MVB cargo sorting. Bars represent the means of four biological replicates each. Cps1, carboxypeptidase S.

expression of $vps9^{M419D}$ or $vps9\Delta^{CUE}$ alleles, which cannot bind ubiquitin, and by the single point-mutant $vps9^{D251A}$ and $vps9^{E288A}$ alleles, which are partially GEF deficient in vitro. In contrast, the double point-mutant $vps9^{D251A,E288A}$ allele, which has no GEF activity in vitro (Keren-Kaplan *et al.*, 2012), showed no improvement in *vps9*Δ *muk1*Δ cells and only marginally improved CPY-Inv sorting in *vps9*Δ *MUK1* cells (Figure 4B; one-way analysis of variance [ANOVA], $p < 0.01$).

We further examined the transport of carboxypeptidase S (Cps1), an archetypal transmembrane protein cargo sorted by ESCRTs into ILVs at MVBs (Odorizzi *et al.*, 1998). Cps1 sorting was quantified using luciferase reporter of intraluminal deposition (LUCID), which monitors the lumenal sequestration of firefly luciferase fused to the cytosolic domain of an MVB cargo protein (Nickerson *et al.*, 2012). Consistent with LUCID assays of another MVB cargo, Sna3 (Paulsel *et al.*, 2013), *vps9*Δ cells exhibited a defect in MVB sorting, as indicated by a fourfold increase in signal from Cps1 fused on its cytosolic domain to firefly luciferase (FLuc; Figure 4C). In contrast, double-mutant *vps9*Δ *muk1*Δ cells had ~20-fold increase in FLuc-Cps1 signal, similar to the level of cargo missorting observed in *vps4*Δ cells, which lack a functional MVB pathway (Figure 4D). As in the thermotolerance and CPY-Inv sorting assays, the CUE-domain mutations ($vps9^{M419D}$ and $vps9\Delta^{CUE}$) and the single point mutations that partially disable Vps9 GEF activity ($vps9^{D251A}$ and $vps9^{E288A}$) caused no reduction in FLuc-Cps1 sorting, whereas the double point-mutant $vps9^{D251A,E288A}$ allele, which lacks detectable GEF activity in vitro (Keren-Kaplan *et al.*, 2012), was only able to modestly support FLuc-Cps1 sorting via the MVB pathway when Muk1 was also expressed (Figure 4, C and D; one-way ANOVA, $p < 0.01$).

Fusion of the CUE domain to Muk1 rescues loss of Vps9 function at late endosomes

Vps9 has a more important role than does Muk1 in late endosomal biogenesis (Figure 1) and in the sorting of protein cargoes through late endosomes (Figure 4; Paulsel *et al.*, 2013). Muk1 lacks a CUE domain, and, in contrast to Vps9, GFP-tagged Muk1 fails to localize to endosomal class E compartments (Paulsel *et al.*, 2013). Given that the CUE domain targets Vps9 to late endosomal membranes (Figure 2), we asked whether a chimeric CUE-Muk1 fusion protein might restore late endosomal functions in *vps9*Δ cells. Fluorescence microscopy confirmed that a GFP-tagged CUE-Muk1 chimera exhibited the same localization pattern seen for GFP-Vps9 (Figure 2), with

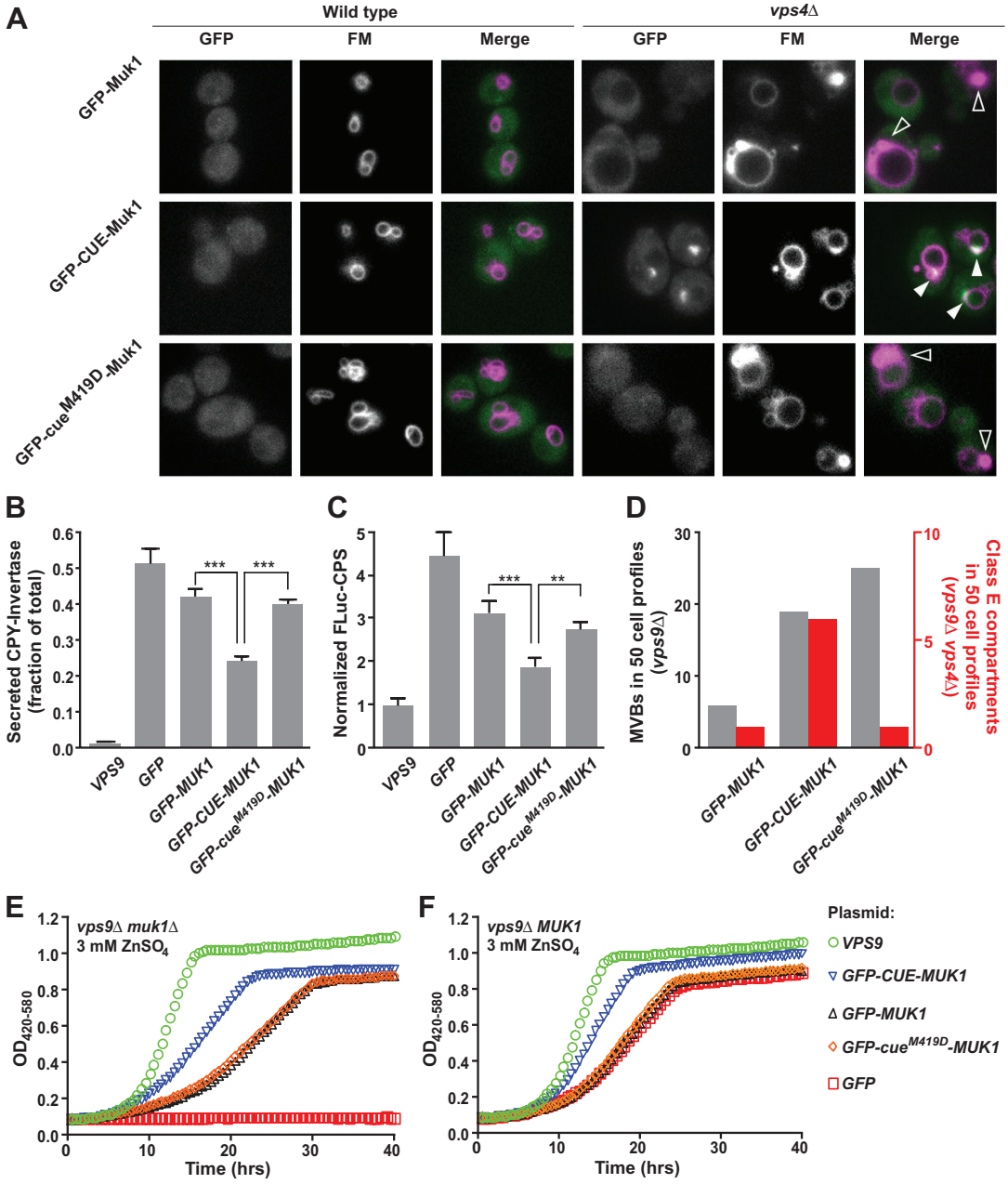

FIGURE 5: Fusion of the CUE domain to Muk1 rescues Vps9 function at late endosomes. (A) Fluorescence micrographs of FM 4-64–stained cells expressing GFP-Muk1 chimeras from a *CEN* plasmid. Arrowheads indicate FM 4-64–labeled class E compartments at which GFP either does (closed arrowheads) or does not (open arrowheads) colocalize. (B) Quantification of CPY-Inv in extracellular and total cellular fractions from *vps9*Δ cells expressing the indicated alleles from a *CEN* plasmid. Bars represent means of three independent biological replicates each. Unpaired one-way ANOVA: $p < 0.0001$ overall; ***$p < 0.001$. (C) LUCID quantification of luciferase-tagged Cps1 in *vps9*Δ cells expressing the indicated alleles from a *CEN* plasmid. Bars represent means of four independent biological replicates each. Unpaired one-way ANOVA: $p < 0.0001$ overall; **$p < 0.01$; ***$p < 0.001$. (D) EM quantification of MVBs (black) and class E compartments (red) in 50 cell profiles. (E, F) Growth curves of yeast lacking both Rab5 GEFs (E) or only Vps9 (F) carrying plasmid-borne *VPS9* or alleles of *MUK1*. Cells were shaken at 30°C in synthetic medium supplemented with 3 mM zinc sulfate. Plotted points represent the mean value of three replicate cultures each.

GFP-CUE-Muk1 being predominantly cytosolic in wild-type yeast but concentrated at class E compartments in *vps4*Δ cells (Figure 5A). This localization pattern was not seen for GFP fused to Muk1 alone or for the mutant GFP-CUE^{M419D}-Muk1 chimera, in which ubiquitin binding by the CUE domain was impaired (Figure 5A). The CUE domain therefore redirects Muk1 to late endosomes in a manner dependent upon ubiquitin binding.

To test whether the CUE-Muk1 chimera could functionally replace Vps9 at late endosomes, we assayed the vacuolar protein sorting and MVB pathways. Whereas expression of GFP-MUK1 from a low-copy plasmid marginally rescued both the CPY-Inv (Figure 5B) and FLuc-Cps1 (Figure 5C) sorting defects seen in *vps9*Δ *MUK1* cells, low-copy expression of GFP-CUE-Muk1 produced a substantial improvement in trafficking of both cargoes compared with

expression of either GFP-Muk1 or the GFP-CUE^{M419D}-Muk1 mutant chimera that cannot bind ubiquitin. We further tested chimeric Muk1 proteins for their ability to support Rab5-dependent stress tolerance by growing cells in media supplemented with 3 mM zinc. Zinc is primarily stored in the yeast vacuole, and zinc sensitivity is a classic indicator of endolysosomal malfunction (Cyert and Philpott, 2013). In cells lacking both Rab5 GEFs (Figure 5E) or only Vps9 (Figure 5F), GFP-CUE-Muk1 substantially rescued sensitivity to zinc, whereas expression of GFP-CUE^{M419D}-Muk1 conferred no more rescue than did GFP-Muk1. These quantitative cargo-sorting and stress-tolerance data indicate that ubiquitin binding by the Muk1 chimera enhances its ability to support Rab5-dependent endolysosomal biogenesis and transport.

The CUE domain has been shown to dimerize in vitro (Prag *et al.*, 2003). To address the possibility that a CUE-domain chimera might improve Muk1 function by promoting dimerization, we fused Muk1 to glutathione *S*-transferase (GST), which also dimerizes (Parker *et al.*, 1990). However, GFP-GST-Muk1 provided no functional rescue of phenotypic defects in *vps9*Δ *muk1*Δ mutants (unpublished data), indicating a general loss of Muk1 function. Similarly, fusion of Muk1 to the FYVE domain, which drives endosomal localization through its interaction with phosphatidylinositol 3-phosphate (Burd and Emr, 1998), also rendered Muk1 nonfunctional (unpublished data). Disruption of Muk1 function upon its fusion to the FYVE domain or to GST might indicate that Muk1 is limited in what type of domain it will tolerate as a chimera. Its tolerance of attachment to the CUE domain, whether or not the CUE domain binds ubiquitin, would be consistent with juxtaposition of the CUE domain and VPS9 domain in the Vps9 protein. In either case, the localization of GFP-CUE-Muk1 to endosomes and the obvious improvements in supporting Vps9-dependent endosomal traffic when this chimeras is able to bind ubiquitin best support a model in which the CUE domain acts as a localization determinant to direct this Rab5 GEF to ubiquitin-replete endosomes.

Expression of GFP-CUE-Muk1, but not GFP-Muk1, also restored the abundance of MVBs in *vps9*Δ mutant cells to the level seen in wild-type cells (Figure 5D), again showing that the CUE domain can confer upon Muk1 a gain of function that replaces the need for Vps9 activity at late endosomes. This point was even more strongly supported by our observation that GFP-CUE-Muk1 expression in *vps4*Δ *vps9*Δ cells restored the formation of class E compartments (Figure 5D), which is a process that depends much more critically on Vps9 activity than does MVB biogenesis (Figure 1). The $M_{419}D$ mutation that disrupts CUE domain binding to ubiquitin (Prag *et al.*, 2003) prevented the GFP-CUE-Muk1 chimera from fully restoring class E compartment formation in *vps4*Δ *vps9*Δ cells (Figure 5D) but had no effect on the ability of GFP-CUE-Muk1 to rescue MVB biogenesis in *vps9*Δ cells (Figure 5D). This observation reinforces the concept that ubiquitin accumulation at late endosomes resulting from ESCRT dysfunction serves to recruit Vps9, which would drive hyperactivation of Vps21 needed for endosomal membrane accumulation at class E compartments beyond what is normally required for MVB biogenesis (Russell *et al.*, 2012).

DISCUSSION

Vps9 was established as a Rab5 GEF in the vacuolar protein sorting pathway of yeast more than 15 years ago (Burd *et al.*, 1996; Hama *et al.*, 1999), but its role in endosome biogenesis was not clear because deletion of the *VPS9* gene caused a relatively mild defect in the sorting of soluble vacuolar enzymes from the Golgi via endosomes (Raymond *et al.*, 1992) and the sorting of transmembrane protein cargoes into ILVs of late endosomal MVBs (Nickerson *et al.*, 2012; Paulsel *et al.*, 2013). The obscurity in understanding the role of Vps9 is explained, in part, by the function of Muk1, a Vps9 homologue that also has GEF activity toward Rab5 paralogues (Cabrera *et al.*, 2013; Paulsel *et al.*, 2013). Our EM studies now show that Vps9 is the primary Rab5 GEF at late endosomes because the biogenesis of MVBs is strongly reduced in the absence of Vps9 and almost completely eliminated when both Vps9 and Muk1 are absent, whereas MVB biogenesis is unaffected in the absence of Muk1 alone.

The importance of Vps9 function at late endosomes was emphasized further by our finding that deletion of the *VPS9* gene abrogated the formation of class E compartments. These aberrant late endosomal structures are seen only when ESCRT function has been disabled, and their formation depends critically upon activation of the Vps21 Rab5 paralogue (Russell *et al.*, 2012). Of importance, we demonstrate that class E compartment formation in ESCRT-mutant cells was abrogated by point mutations shown in vitro to disable Vps9 GEF activity toward Vps21 (Keren-Kaplan *et al.*, 2012), which highlights the critical role of Vps9 in driving the hyperactivation of Vps21 that occurs in response to ESCRT dysfunction (Russell *et al.*, 2012). That the same point mutations did not completely abolish MVB biogenesis in cells that have wild-type ESCRT activity is consistent with Muk1-mediated activation of Vps21 (or other Rab5 paralogues) being sufficient to sustain endolysosomal membrane trafficking at a residual rate when Vps9 is absent (Paulsel *et al.*, 2013). However, class E compartment formation relies on hyperactivation of Vps21 for driving endosomal membrane fusion beyond levels normally required for MVB biogenesis (Russell *et al.*, 2012), and our finding that Muk1 is not sufficient for this process emphasizes the importance of Vps9 function in late endosome biogenesis and that this function only partially overlaps that of Muk1.

The inability of Muk1 to replace Vps9 function can be explained in part by the CUE domain, which is found in Vps9 but not Muk1. However, despite the role that the CUE domain has in binding to ubiquitin (Prag *et al.*, 2003), its specific contribution to Vps9 function was unclear because deletion of this region causes virtually no trafficking defects (Davis *et al.*, 2003; Prag *et al.*, 2003). Our study finds that ubiquitin binding by the CUE domain is chiefly responsible for mediating the localization of Vps9 to late endosomes. That the CUE domain is not essential for endosomal trafficking (Davies *et al.*, 2003; Prag *et al.*, 2003; this study), however, suggests that residual endosomal localization occurs independently of the CUE domain, which we occasionally observed with ubiquitin-binding Vps9 mutants. Similarly, mammalian Rabex-5 is targeted to endosomes not solely through ubiquitin-binding motifs but also by a predicted coiled-coil motif that more weakly mediates endosomal localization (Mattera and Bonifacino, 2008). The central VPS9 domain common to Vps9 and Rabex-5 might help promote targeting to endosomes, which would be consistent with the observation that the VPS9 domain from RABX-5 of *Caenorhabditis elegans* localizes to endosomes when expressed in yeast (Poteryaev *et al.*, 2010).

Our finding that fusion of the Vps9 CUE domain to Muk1 rescued protein sorting and MVB biogenesis in cells lacking Vps9 supports the concept that the CUE domain, through its function as a localization determinant, promotes Vps9 activation of Rab5 activity at membranes enriched in ubiquitinated proteins (Carney *et al.*, 2006). This role was even more strongly emphasized by our finding that the CUE domain endowed Muk1 with the ability to replace Vps9 function in class E compartment formation. That the $M_{419}D$ mutation, which disables ubiquitin binding, abolished the ability of the CUE-Muk1 chimera to rescue protein sorting but did not prevent its rescue of MVB biogenesis suggests a role beyond ubiquitin binding through which the CUE domain promotes Vps9 function at

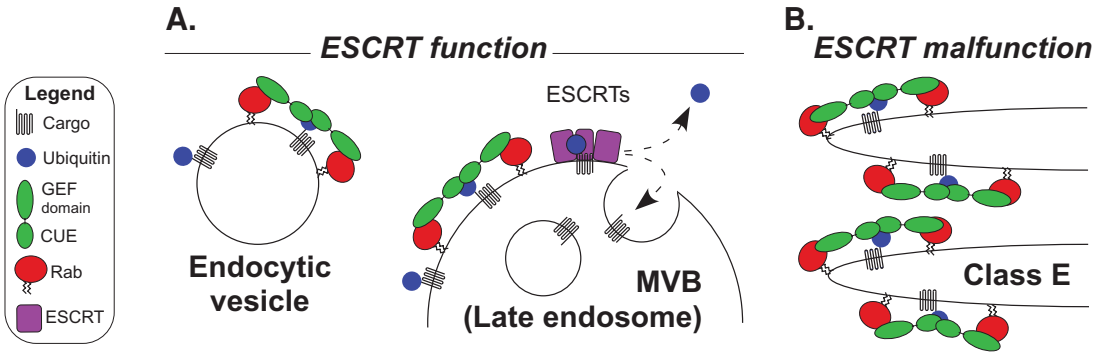

FIGURE 6: Model of ubiquitin-mediated recruitment of Vps9 to endosomes. (A) During normal endosomal transport, the CUE domain of Vps9 promotes recruitment of Vps9 to endosomes and endocytic vesicles through interaction with ubiquitinated transmembrane cargo proteins, thereby promoting Vps21 nucleotide exchange and endosomal localization. Dimerization of the Vps9 CUE domain might increase Vps9 recruitment to endosomes. Sorting and deubiquitination of cargo by ESCRTs reduces ubiquitin at the endosomal surface, promoting the dissociation of Vps9. (B) Disruption of ESCRT function leads to an accumulation of ubiquitinated cargo at the endosomal surface, thereby aberrantly maintaining Vps9 at endosomes and prolonging Vps21 activity. Vps9-mediated Vps21 hyperactivation leads to the increased endosomal membrane fusion that creates class E compartments.

late endosomes. However, the $M_{419}D$ mutation inhibited the ability of the CUE-Muk1 chimera to generate class E compartments, consistent with ubiquitin binding by Vps9 having a major role in driving the hyperactivation of Vps21 that occurs upon ESCRT dysfunction (Russell *et al.*, 2012). In vitro, the Vps9 CUE domain forms a dimer that binds one ubiquitin (Prag *et al.*, 2003), which might explain why Vps9 accumulates so dramatically at class E compartments, where ubiquitin also accumulates (Ren *et al.*, 2008). Whereas it is appealing to speculate that Vps21 activity is sustained at endosomes by Vps9 until ubiquitin is removed through ESCRT-mediated sorting of cargoes into the MVB pathway, several aspects of this model require further testing.

The GEF activities of both Rabex5 and Vps9 are boosted by truncation of their respective ubiquitin-binding domains, consistent with ubiquitin binding being inhibitory (Delparato *et al.*, 2004; Keren-Kaplan *et al.*, 2012). An increase in Vps9 activity upon mutation of its CUE domain might explain why class E compartment formation, which critically depends on Vps9 GEF activity, was not disabled by CUE-domain mutations, despite the reduction in endosomal localization of Vps9. Both mammalian Rabex-5 and yeast Vps9 are ubiquitinated in vivo, which had suggested a model in which autoinhibitory ubiquitin binding in-*cis* is relieved by intermolecular interactions in-*trans* between Rabex-5 and ubiquitinated transmembrane proteins trafficking through the endolysosomal pathway (Mattera and Bonifacino, 2008). However, reconstitution of Vps9 ubiquitination in vitro did not inhibit the nucleotide exchange activity Vps9 has toward Vps21 (Keren-Kaplan *et al.*, 2012), although additional factors might exist in vivo that regulate Vps9 activity. A model in which Vps9 autoinhibitory ubiquitin-binding is displaced by interactions in-*trans* between the CUE domain and ubiquitinated transmembrane proteins that accumulate at class E compartments could contribute to the amplification of Vps21 signaling upon ESCRT dysfunction (Russell *et al.*, 2012), although at present, testing this model is difficult. Our data are at least consistent with ubiquitin accumulation at class E compartments promoting Vps21 hyperactivation by amplified recruitment of Vps9 to endosomes (Figure 6). A role for ubiquitin accumulation in driving the formation of class E compartments is also supported by the suppression of class E compartment formation observed upon overexpression of the *DOA4* gene (Luhtala and Odorizzi, 2004), which encodes the ubiquitin hydrolase that deubiquitinates transmembrane proteins sorted at MVBs (Dupré and Haguenauer-Tsapis, 2001; Katzmann *et al.*, 2001; Reggiori and Pelham, 2001). The deubiquitination of transmembrane proteins sorted by ESCRTs would remove the ubiquitin signal that recruits and/or retains Vps9 (Figure 6). The dissociation of Vps9 would permit the Msb3 GAP to terminate Vps21/Rab signalingVps21/Rab5 signaling, as early endosomes mature into late endosomes (Lachmann *et al.*, 2012; Nickerson *et al.*, 2012).

MATERIALS AND METHODS

Yeast strains and plasmid construction

Standard procedures were used for manipulating *S. cerevisiae* (Guthrie and Fink, 2002) and for DNA manipulations using *Escherichia coli* (Sambrook and Russell, 2001). Strains are shown in Table 1 and plasmids in Table 2. Plasmids were confirmed by DNA sequence analysis. Gene deletions and chromosomal integrations in yeast were constructed by homologous recombination using site-specific cassettes that were amplified by PCR (Longtine *et al.*, 1998; Gueldener *et al.*, 2002). The low-copy yeast shuttle plasmid pDN614 was made essentially as described for pDN616 (Nickerson *et al.*, 2012). All luciferase plasmids used in this study carry the *PGK1pr::RLuc::GCY1tr* gene cassette cloned into the *Xho*I restriction site of pDN616 or pDN614, as described (Nickerson *et al.*, 2012). LUCID plasmid pDN278 expressing FLuc-tagged Cps1 under its native promoter was constructed via two cloning steps: first, the *CPS1* promoter (500 base pairs) and *FLuc* coding sequences were joined by PCR sequence overlap extension (SOE) and integrated by homologous recombination into the SacII-digested *RLuc* plasmid; second, a unique *Sac*II site introduced after the *FLuc* coding sequence allowed in-frame integration by homologous recombination of a PCR product containing the *CPS1* coding sequence and 192 base pairs of native *CPS1* terminator sequence. For constructing the LUCID Cps1 plasmid pDN336, the polylinker of pDN278, containing both *RLuc* and *FLuc-CPS1* inserts, was isolated by digestion with *Pvu*II, and the resulting fragment was cloned into *Xho*I/*Sac*I-digested pDN614. Chimeras of Muk1 and CUE-domain alleles of Vps9 were constructed by PCR SOE to link *VPS9* codons 408–451 in-frame with the coding region of *MUK1*, followed by 291 base pairs of native *MUK1* terminator. PCR templates for wild-type and $M_{419}D$ alleles of the CUE domain were from plasmids reported

Name	Genotype	Reference/ source
SEY6210	*MATa leu2-3112 ura3-52 his3200 trp1901 lys2801 suc29*	Robinson *et al.* (1988)
BHY10	SEY6210; *leu2-3112::pBHY11 (CPY-INV::LEU2)*	Horazdovsky *et al.* (1994)
MBY3	SEY6210; *vps4Δ::TRP1*	Babst *et al.* (1997)
GOY223	BHY10; *vps9Δ::HIS3*	This study
GOY224	BHY10; *vps9Δ::HIS3 vps4Δ::TRP1*	This study
DNY516	BHY10; *muk1Δ::KANMX6*	Paulsel *et al.* (2013)
DNY517	BHY10; *muk1Δ::KANMX6 vps9Δ::HIS3*	Paulsel *et al.* (2013)
TSY23	BHY10; *muk1Δ::KANMX6 vps4::TRP1*	This study

TABLE 1: Yeast strains used in this work.

Name	Genotype	Reference/ source
pRS416	*URA3 Amp^R CEN/ARSH4*	Sikorski and Hieter (1989)
pRS426	*URA3 Amp^R 2 μ*	Sikorski and Hieter (1989)
pBD1	*URA3 Amp^R* (pRS416) *VPS9*	Davies (2003)
pBD3	*URA3 Amp^R* (pRS416) *vps9Δ^{CUE}*	Davies (2003)
pBD4	*URA3 Amp^R* (pRS416) *vps9^{M419D}*	Davies (2003)
pGO656	*URA3 Amp^R* (pRS416) *vps9^{D251A}*	This study
pGO741	*URA3 Amp^R* (pRS416) *VPS9^{E288A}*	This study
pGO763	*URA3 Amp^R* (pRS416) *VPS9$^{D251A/E288A}$*	This study
pCB243	*URA3 Amp^R* (pRS426) *GFP-VPS9*	This study
pGO678	*URA3 Amp^R* (pRS426) *GFP-vps9Δ^{CUE}*	This study
pGO730	*URA3 Amp^R* (pRS426) *GFP-vps9^{M419D}*	This study
pGO723	*URA3 Amp^R* (pRS426) *GFP-vps9-CUE*	This study
pGO729	*URA3 Amp^R* (pRS426) *GFP-vps9-CUE^{M419D}*	This study
pTS25	*URA3 Amp^R* (pRS426) *GFP-vps9^{NT}*	This study
pTS28	*URA3 Amp^R* (pRS426) *GFP-vps9^{VND}*	This study
pDN616	*URA3 Amp^R LoxP::CEN/ ARSH4::LoxP*	Nickerson *et al.* (2012)
pDN278	*PGK1$_{pr}$::RLuc CPS1$_{pr}$::FLuc-CPS* (pDN616)	This study
pDN614	*Amp^R TRP1 LoxP::CEN/ ARSH4::LoxP*	This study
pDN336	*PGK1$_{pr}$::RLuc CPS1$_{pr}$::FLuc-CPS* (pDN614)	This study
pGO36	*Amp^R URA3 CEN/ARSH4 CPY$_{pr}$::GFP*	Odorizzi *et al.* (1998)
pDN219	*CPY$_{pr}$::GFP-MUK1* (pGO36)	Paulsel *et al.* (2013)
pDN344	*CPY$_{pr}$::GFP-vps9CUE-MUK1* (pGO36)	This study
pDN345	*CPY$_{pr}$::GFP-vps9cue^{M419D}-MUK1* (pGO36)	This study

TABLE 2: Plasmids used in this work.

in Davies *et al.* (2003). PCR products for chimeras were cloned via homologous recombination into the *Bgl*II-digested GFP fusion plasmid pGO36 (Odorizzi *et al.*, 1998), which resulted in the insertion of *CUE-MUK1* alleles downstream of, and in-frame with, the *GFP* reading frame.

Fluorescence microscopy

Yeast were grown to logarithmic phase at 30°C and stained with FM 4-64 (Life Technologies, Carlsbad, CA), using a pulse-chase procedure as previously described (Odorizzi, 2003). Cells were labeled in 50 μl of yeast extract/peptone/dextrose (YPD) supplemented with 30 nM FM 4-64 for 20 min at 30°C and then washed with 1 ml of YPD and chased in 5 ml of YPD. Labeled cells were washed and resuspended in yeast nitrogen base synthetic minimal medium and then placed under coverslips on glass slides for viewing. Confocal fluorescence microscopy shown in Figure 2 was performed using an inverted fluorescence microscope (TE2000-U; Nikon, Melville, NY) equipped with an electron-multiplying charge-coupled device camera (Cascade II; Photometrics, Tucson, AZ) and a Yokogawa spinning disk confocal system (CSU-Xm2; Nikon); these images were taken with a 100×/numerical aperture 1.4 oil objective and acquired using MetaMorph, version 7.0 (MDS Analytical Technologies, Sunnyvale, CA). Fluorescence intensity measurements were made on unaltered image files using ImageJ software (National Institutes of Health, Bethesda, MD). Fluorescence intensity ratios were calculated as the ratio of FM 4-64–colocalized GFP to an area of cytosolic GFP. At least 10 cells were analyzed for each sample, and ratios were analyzed using GraphPad (San Diego, CA) Prism software by unpaired ANOVA with Bonferroni correction. Fluorescence microscopy shown in Figure 5 was performed as described (Paulsel *et al.*, 2013). All images were processed using Photoshop CS3 or CS6 software (Adobe Systems, San Jose, CA).

Electron microscopy

Yeast cells grown to logarithmic phase at 30°C were transferred to aluminum planchettes and frozen in a Wohlwend Compact 02 High Pressure Freezer. Planchettes were transferred to vials containing freeze substitution solution (0.1% uranyl acetate, 2% glutaraldehyde in anhydrous acetone). Vials were transferred to a freeze substitution machine (EM AFS2; Leica, Vienna, Austria) at –140°C. Samples were warmed to –80°C over 24 h, and then the cells were removed from the planchettes and transferred to chilled tubes, in which the freeze substitution solution replaced. After 48 h, samples were warmed to –60°C. Over the next 96 h, samples were washed thrice with acetone and then 1:3, 1:1, and 3:1 acetone/Lowicryl HM20 (Polysciences, Warrington, PA), followed by six washes with HM20. The HM20 was polymerized under ultraviolet light as it warmed to 20°C over 48 h. A Leica ultramicrotome was used to cut 90-nm sections, which were collected onto 1% Formvar films adhered to rhodium-plated copper grids (Electron Microscopy Sciences, Hatfield, PA). Sections were then poststained in 2% uranyl acetate for 10 min and in Reynold's lead citrate for 20 min before being imaged using a Philips CM10

transmission electron microscope at 80 kV. Images were processed using Adobe CS3 software. For quantification, MVBs were morphologically defined as spherical structures surrounded by a discernible bilayer and containing at least two ILVs. class E compartments were defined as two or more contacting cisternae, each of which had a length at least twice as long as it its width.

Cargo-trafficking assays

Colorimetric quantification of extracellular and total cellular CPY-Inv was performed essentially as described (Darsow *et al.*, 2000). Overnight cultures of cells expressing a chromosomal integration of CPY-Inv were diluted in selective synthetic media with 2% fructose and 0.05% (wt/vol) casamino acids and shaken at 30°C for ~6 h and analyzed in log phase (OD_{600} of 0.4–1.0). Total cellular CPY-Inv activity was determined by lysing 50% of each sample by addition of 1% (vol/vol) Triton X-100 with two rounds of freeze-thaw in liquid nitrogen.

Quantitative analysis of MVB cargo sorting by LUCID was performed using a dual luciferase assay system (Promega, Madison, WI) essentially as described (Nickerson *et al.*, 2012). The luciferase epitope was fused to the cytosolic N-terminus of Cps1. Overnight cultures were diluted in selective synthetic media with 2% glucose and 0.05% (wt/vol) casamino acids and shaken at 30°C for ~5 h and analyzed in log phase (OD_{600} of 0.4–1.0). A 20-min cycloheximide treatment (50 µg/ml) preceded collection of ~1.2 OD_{600} cells, which were lysed in 200 µl of lysis buffer by vortexing with glass beads. FLuc and *Renilla* luciferase (RLuc) were analyzed sequentially in opaque 96-well plates using a PerkinElmer (Waltham, MA) Victor Light Model 1420 luminometer equipped with automated injectors. Signal from FLuc-Cps1 was normalized versus signal from soluble RLuc expressed from the same plasmid.

Statistical analyses of cargo sorting assays were performed using Microsoft Excel and GraphPad Prism software. Paired and unpaired ANOVA used the Tukey multiple comparisons test.

Western blotting

Total yeast extracts were generated from five OD_{600} units of logarithmically grown cells that were harvested by centrifugation at 500 × *g*, resuspended in 10% (vol/vol) trichloroacetic acid, and incubated for 30 min on ice. Protein precipitates were isolated by centrifugation at 15,000 × *g* for 10 min at 4°C, and the insoluble material was reprecipitated twice by sonication into ice-cold acetone and centrifugation before being sonicated into Laemmli buffer. One-half OD_{600} unit of extract was resolved by SDS–PAGE and examined by Western blotting, which was performed by chemiluminescence and film exposure. Anti-GFP monoclonal mouse antibody was procured from Roche Diagnostics (Basel, Switzerland).

Growth assays

Yeast growth kinetics was monitored using a Bioscreen-C plate reading incubator (Growth Curves USA, Piscataway, NJ). Cultures of selective growth media, 150 µl (2% glucose, 0.05% casamino acids), with or without 3 mM $ZnSO_4$ were shaken at 30°C. To prevent clumping of cells commonly seen when using synthetic media in Bioscreen-C 100-well plates, Nonidet-P40 was added to 0.2% (vol/vol; McIntosh *et al.*, 2011). To keep zinc soluble in synthetic media, ammonium sulfate was replaced by asparagine at molar equivalence to omitted ammonium.

ACKNOWLEDGMENTS

We thank Thomas Giddings for EM support and Gia Voeltz for stimulating discussions (both at the University of Colorado, Boulder, CO). Chris Burd (Yale University) kindly provided plasmid pCB243. D.P.N. is an American Cancer Society Postdoctoral Fellow. This work was funded by National Institutes of Health Grants R01GM-111335 to G.O. and R01 GM077349 to A.J.M.

REFERENCES

Babst M, Sato TK, Banta LM, Emr SD (1997). Endosomal transport function in yeast requires a novel AAA-type ATPase, Vps4p. EMBO J 16, 1820–1831.

Bankaitis VA, Johnson LM, Emr SD (1986). Isolation of yeast mutants defective in protein targeting to the vacuole. Proc Natl Acad Sci USA 83, 9075–9079.

Barr F, Lambright DG (2010). Rab GEFs and GAPs. Curr Opin Cell Biol 22, 461–470.

Burd CG, Emr SD (1998). Phosphatidylinositol (3)-phosphate signaling mediated by specific binding to RING FYVE domains. Mol Cell 2, 157–162.

Burd CG, Mustol PA, Schu PV, Emr SD (1996). A yeast protein related to a mammalian Ras-binding protein, Vps9p, is required for localization of vacuolar proteins. Mol Cell Biol 16, 2369–2377.

Cabrera M, Arlt H, Epp N, Lachmann J, Griffith J, Perz A, Reggiori F, Ungermann C (2013). Functional separation of endosomal fusion factors and the class C core vacuole/endosome tethering (CORVET) complex in endosome biogenesis. J Biol Chem 288, 5166–5175.

Carney DS, Davies BA, Horazdovsky BF (2006). Vps9 domain-containing proteins: activators of Rab5 GTPases from yeast to neurons. Trends Cell Biol 16, 27–35.

Cyert MS, Philpott CC (2013). Regulation of cation balance in Saccharomyces cerevisiae. Genetics 193, 677–713.

Darsow T, Odorizzi G, Emr SD (2000). Invertase fusion proteins for analysis of protein trafficking in yeast. Methods. Enzymol 327, 95–106.

Davies BA, Topp JD, Sfeir AJ, Katzmann DJ, Carney DS, Tall GG, Friedberg AS, Deng L, Chen Z, Horazdovsky BF (2003). Vps9p CUE domain ubiquitin binding is required for efficient endocytic protein traffic. J Biol Chem 278, 19826–19833.

Delprato A, Merithew E, Lambright DG (2004). Structure, exchange determinants, and family-wide rab specificity of the tandem helical bundle and Vps9 domains of Rabex-5. Cell 118, 607–617.

Donaldson KM, Yin H, Gekakis N, Supek F, Joazeiro CAP (2003). Ubiquitin signals protein trafficking via interaction with a novel ubiquitin binding domain in the membrane fusion regulator, Vps9p. Curr Biol 13, 258–262.

Dupré S, Haguenauer-Tsapis R (2001). Deubiquitination step in the endocytic pathway of yeast plasma membrane proteins: crucial role of Doa4p ubiquitin isopeptidase. Mol Cell Biol 21, 4482–4494.

Giddings TH, O'Toole ET, Morphew M, Mastronarde DN, McIntosh JR, Winey M (2001). Using rapid freeze and freeze-substitution for the preparation of yeast cells for electron microscopy and three-dimensional analysis. Methods Cell Biol 67, 27–42.

Gueldener U, Heinisch J, Koehler GJ, Voss D, Hegemann JH (2002). A second set of loxP marker cassettes for Cre-mediated multiple gene knockouts in budding yeast. Nucleic Acids Res 30, e23.

Guthrie C, Fink GR (2002). Methods in Enzymology: Guide to Yeast Genetics and Molecular and Cell Biology, Academic Press.

Hama H, Tall GG, Horazdovsky BF (1999). Vps9p is a guanine nucleotide exchange factor involved in vesicle-mediated vacuolar protein transport. J Biol Chem 274, 15284–15291.

Hanson PI, Cashikar A (2012). Multivesicular body morphogenesis. Annu Rev Cell Dev Biol 28, 337–362.

Horazdovsky BF, Busch GR, Emr SD (1994). VPS21 encodes a rab5-like GTP binding protein that is required for the sorting of yeast vacuolar proteins. EMBO J 13, 1297–1309.

Horiuchi H, Lippé R, McBride HM, Rubino M, Woodman P, Stenmark H, Rybin V, Wilm M, Ashman K, Mann M, *et al.* (1997). A novel Rab5 GDP/GTP exchange factor complexed to Rabaptin-5 links nucleotide exchange to effector recruitment and function. Cell 90, 1149–1159.

Katzmann DJ, Babst M, Emr SD (2001). Ubiquitin-dependent sorting into the multivesicular body pathway requires the function of a conserved endosomal protein sorting complex, ESCRT-I. Cell 106, 145–155.

Keren-Kaplan T, Attali I, Motamedchaboki K, Davis BA, Tanner N, Reshef Y, Laudon E, Kolot M, Levin-Kravets O, Kleifeld O, *et al.* (2012). Synthetic biology approach to reconstituting the ubiquitylation cascade in bacteria. EMBO J 31, 378–390.

Lachmann J, Barr FA, Ungermann C (2012). The Msb3/Gyp3 GAP controls the activity of the Rab GTPases Vps21 and Ypt7 at endosomes and vacuoles. Mol Biol Cell 23, 2516–2526.

Longtine MS, McKenzie A, Demarini DJ, Shah NG, Wach A, Brachat A, Philippsen P, Pringle JR (1998). Additional modules for versatile and economical PCR-based gene deletion and modification in Saccharomyces cerevisiae. Yeast 14, 953–961.
Luhtala N, Odorizzi G (2004). Bro1 coordinates deubiquitination in the multivesicular body pathway by recruiting Doa4 to endosomes. J Cell Biol 166, 717–729.
Mattera R, Bonifacino JS (2008). Ubiquitin binding and conjugation regulate the recruitment of Rabex-5 to early endosomes. EMBO J 27, 2484–2494.
Mattera R, Tsai YC, Weissman AM, Bonifacino JS (2006). The Rab5 guanine nucleotide exchange factor Rabex-5 binds ubiquitin (Ub) and functions as a Ub ligase through an atypical Ub-interacting motif and a zinc finger domain. J Biol Chem 281, 6874–6883.
McIntosh KB, Bhattacharya A, Willis IM, Warner JR (2011). Eukaryotic cells producing ribosomes deficient in Rpl1 are hypersensitive to defects in the ubiquitin-proteasome system. PLoS One 6, e23579.
Nickerson DP, Russell MR G, Lo S-Y, Chapin HC, Milnes JM, Merz AJ (2012). Termination of isoform-selective Vps21/Rab5 signaling at endolysosomal organelles by Msb3/Gyp3. Traffic 13, 1411–1428.
Odorizzi G (2003). Bro1 is an endosome-associated protein that functions in the MVB pathway in Saccharomyces cerevisiae. J. Cell Sci 116, 1893–1903.
Odorizzi G, Babst M, Emr SD (1998). Fab1p PtdIns(3)P 5-kinase function essential for protein sorting in the multivesicular body. Cell 95, 847–858.
Parker MW, Lo Bello M, Federici G (1990). Crystallization of glutathione *S*-transferase from human placenta. J Mol Biol 20, 221-222.
Paulsel AL, Merz AJ, Nickerson DP (2013). Vps9 family protein Muk1 is the second Rab5 guanosine nucleotide exchange factor in budding yeast. J Biol Chem 288, 18162-18171.
Poteryaev D, Datta S, Ackema K, Zerial M, Spang A (2010). Identification of the switch in early-to-late endosome transition. Cell 141, 497–508.
Prag G, Misra S, Jones EA, Ghirlando R, Davies BA, Horazdovsky BF, Hurley JH (2003). Mechanism of ubiquitin recognition by the CUE domain of Vps9p. Cell 113, 609–620.
Raymond CK, Howald-Stevenson I, Vater CA, Stevens TH (1992). Morphological classification of the yeast vacuolar protein sorting mutants: evidence for a prevacuolar compartment in class E vps mutants. Mol Biol Cell 3, 1389–1402.
Reggiori F, Pelham HR (2001). Sorting of proteins into multivesicular bodies: ubiquitin-dependent and -independent targeting. EMBO J 20, 5176–5186.
Ren J, Pashkova N, Winistorfer S, Piper RC (2008). DOA1/UFD3 plays a role in sorting ubiquitinated membrane proteins into multivesicular bodies. J Biol Chem 283, 21599–21611.
Rieder SE, Banta LM, Köhrer K, McCaffery JM, Emr SD (1996). Multilamellar endosome-like compartment accumulates in the yeast vps28 vacuolar protein sorting mutant. Mol Biol Cell 7, 985–999.
Rubino M, Miaczynska M, Lippé R, Zerial M (2000). Selective membrane recruitment of EEA1 suggests a role in directional transport of clathrin-coated vesicles to early endosomes. J Biol Chem 275, 3745–3748.
Robinson JS, Klionsky DJ, Banta LM, Emr SD (1988). Protein sorting in Saccharomyces cerevisiae: isolation of mutants defective in the delivery and processing of multiple vacuolar hydrolases. Mol Cell Biol 8, 4936–4948.
Russell MRG, Shideler T, Nickerson DP, West M, Odorizzi G (2012). Class E compartments form in response to ESCRT dysfunction in yeast due to hyperactivity of the Vps21 Rab GTPase. J Cell Sci 125, 5208–5220.
Sambrook J, Russell DW (2001). Molecular Cloning: A Laboratory Manual, Cold Spring Harbor Laboratory Press.
Shih SC, Prag G, Francis SA, Sutanto MA, Hurley JH, Hicke L (2003). A ubiquitin-binding motif required for intramolecular monoubiquitylation, the CUE domain. EMBO J 22, 1273–1281.
Sikorski RS, Hieter P (1989). A system of shuttle vectors and yeast host strains designed for efficient manipulation of DNA in Saccharomyces cerevisiae. Genetics 122, 19–27.
Singer-Krüger B, Stenmark H, Düsterhöft A, Philippsen P, Yoo JS, Gallwitz D, Zerial M (1994). Role of three rab5-like GTPases, Ypt51p, Ypt52p, and Ypt53p, in the endocytic and vacuolar protein sorting pathways of yeast. J Cell Biol 125, 283–298.
Stenmark H (2009). Rab GTPases as coordinators of vesicle traffic. Nat Rev Mol Cell Biol 10, 513–525.
Uejima T, Ihara K, Goh T, Ito E, Sunada M, Ueda T, Nakano A, Wakatsuki S (2010). GDP-bound and nucleotide-free intermediates of the guanine nucleotide exchange in the Rab5·Vps9 system. J Biol Chem 285, 36689–36697.
Vida TA, Emr SD (1995). A new vital stain for visualizing vacuolar membrane dynamics and endocytosis in yeast. J Cell Biol 128, 779–792.